JOURNAL OF MATERIALS SCIENCE **34** (1999) 35–43

Optimization of the coercivity-modifying hydrogenation and re-calcination processes for strontium hexaferrite powder synthesized conventionally

S. A. S. EBRAHIMI*, C. B. PONTON, I. R. HARRIS
School of Metallurgy and Materials, The University of Birmingham, Edgbaston, Birmingham, B15 2TT, UK

A. KIANVASH
Department of Ceramic Engineering, Faculty of Engineering, The University of Tabriz, Tabriz 51 664, Iran

Strontium hexaferrite powder, synthesised conventionally in-house from strontium carbonate ($SrCO_3$) and hematite (Fe_2O_3) without additives, has been treated in a static hydrogen atmosphere and subsequently calcined in static air under different conditions. The optimum time, temperature, and initial pressure of hydrogenation and the optimum temperature of re-calcination for a fixed time of 1 h were determined using a combination of X-ray diffraction, vibrating sample magnetometer, and high-resolution scanning electron microscope techniques.

Increasing the temperature, initial pressure, and time of hydrogenation up to the determined optimum values resulted in the decomposition of the strontium hexaferrite into Fe_2O_3 and $Sr_7Fe_{10}O_{22}$, together with a more marked reduction of the resultant Fe_2O_3 to Fe. This was accompanied by the conversion of the initial single-crystal particles into very fine sub-grains, which is the reason for the higher coercivities obtained after re-calcination. Increasing the hydrogenation and re-calcination parameters beyond the optimum values, however, generally resulted in grain growth, which decreased the final magnetic properties. Increasing the re-calcination temperature to 1000 °C resulted in completion of the hexaferrite reformation. Beyond this temperature, however, the coercivity decreased due to grain growth.

The optimum conditions were as follows: hydrogenation at 700 °C for 1 h under an initial pressure of 1.3 bar and then re-calcination in air at 1000 °C for 1 h. The highest coercivity obtained after re-calcination was around 400 kA/m. The remanence and saturation magnetization values were very similar to their initial values before the hydrogen treatment. © *1999 Kluwer Academic Publishers*

1. Introduction

A hydrogen atmosphere has previously been employed to introduce iron into Co–Ti–Sn-substituted Ba–ferrite particles by reducing a proportion of the Fe ions to increase the saturation magnetization [1]. Similar work was carried out on Co–Zn–Ti–Sn-substituted Ba–ferrite particles [2]. A new method of processing hexaferrites to produce an increased intrinsic coercivity has now been patented for commercial and hydrothermally synthesized ferrite materials [3, 4]. By this method, low coercivity can be produced by heat-treating the powders in the presence of hydrogen, nitrogen, or carbon. High coercivity can then be achieved by a re-calcination in air. A further study of the effect of the nitrogen on conventionally synthesised strontium hexaferrite was conducted and the achievements of improved intrinsic coercivities confirmed [5]. Subsequently, a detailed study of the phase transformations occurring in commercially sourced strontium hexaferrite powder during dynamic hydrogenation and subsequent re-calcination in static air was carried out and will be reported elsewhere [6].

This work, however, is concerned with the optimization of the various parameters of the hydrogenation treatment, such as temperature, time, and initial pressure, as well as the re-calcination temperature

* Also Department of Metallurgy, Faculty of Engineering, Tehran University, P. O. Box 11365-4563, Tehran, Iran.

and time in order to optimize the magnetic properties of in-house conventionally synthesized strontium hexaferrite. The material has been characterized using X-ray diffraction (XRD), vibrating sample magnetometer (VSM), and high-resolution scanning electron microscope (HRSEM) techniques.

2. Experimental procedure

The starting material was M-type strontium hexaferrite ($SrFe_{12}O_{19}$) produced conventionally in-house by the milling, mixing, and then calcining of strontium carbonate and hematite (α-Fe_2O_3). The milling time before mixing was 3.5 h for iron oxide and 5 h for strontium carbonate. Methanol was used as the milling medium. The ratio of iron oxide to strontium carbonate was 5.5 to 1 without using any additives. The calcination was carried out in a resistance-heated muffle furnace at 1100 °C for 1 h in air [4]. The hydrogenation was performed in a static atmosphere at various initial pressures. The maximum initial pressure of the hydrogen that could be applied in the system was 1.3 bar. The amount of powder in each batch was 4 g. In the hydrogen furnace, i.e., a resistance-heated vacuum tube furnace, the pressure could be monitored using a computer interfaced to the system. Thus, the computer recorded the variations in the hydrogen pressure with time and temperature. The hydrogenation process consisted of heating the powder at a rate of 5 °C/min up to various temperatures, dwelling for various times and then cooling at the same rate [4]. The subsequent re-calcination process involved heating the hydrogenated powder in static air up to various temperatures, dwelling at the temperature for 1 h, and then cooling it. The heating and cooling rate was 5 °C/min and 10 °C/min, respectively. The re-calcination process was performed in a resistance-heated muffle furnace. The treated powder was subjected to a light milling process prior to the measurements. The magnetic properties were measured at room temperature using a VSM operating up to a maximum field of 1100 kA/m. The magnetization at this field is referred to as maximum magnetization (M_m) in this work. The majority part of the VSM samples were mounted in molten wax but were not subjected to a magnetic alignment field and so were magnetically isotropic. On applying a field, there was no evidence of anisotropy in the treated powders. Thermo Magnetic Analysis (TMA) was performed using a Sucksmith balance. XRD (CoK_α radiation) was used for phase identification, while the microstructure and morphology of the particles were studied using a high-resolution Hitachi S-4000 FEG scanning electron microscope (HRSEM).

3. Results and discussion

3.1. Initial as-conventionally synthesised Sr Hexaferrite

The initial conventionally synthesized powder had a gray color. Its magnetization curve is shown in Fig. 1 and its magnetic properties are summarized in Table I.

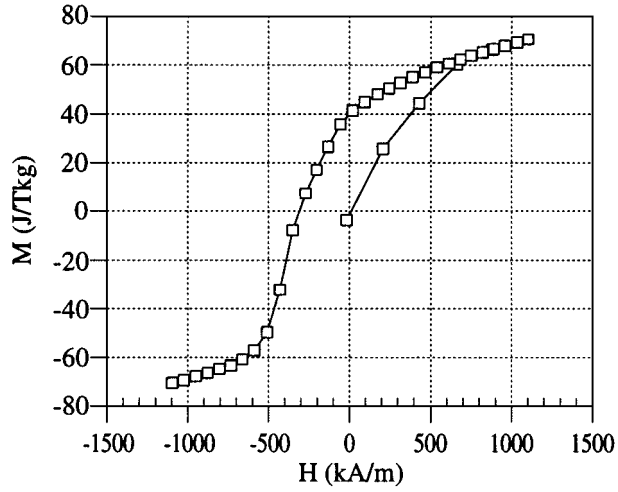

Figure 1 Magnetization curve for the conventionally synthesized starting powder.

TABLE I Magnetic properties of the initial as-conventionally synthesized powder

Sample	Mr (±3%, J/Tkg)	Hci (±2%, kA/m)	Ms (±3%, /Tkg)
Initial	38.1	314.6	67.55
Hydrogenated	5.5	8.6	110.35
Hydrogenated and re-calcined	36.2	390.9	65.45

3.2. Optimized hydrogenation time

The variations in the magnetic properties for the strontium hexaferrite synthesized conventionally, hydrogenated at 850 °C under an initial pressure of 1.3 bar for different times, and subsequently calcined at 1000 °C for 1 h in air are shown in Fig. 2.

Both the remanence (M_r) and maximum magnetization (M_m) show a very small increase with increasing time up to 1 h, followed by a slight decrease. The intrinsic coercivity (H_{ci}) also exhibits a small increase with

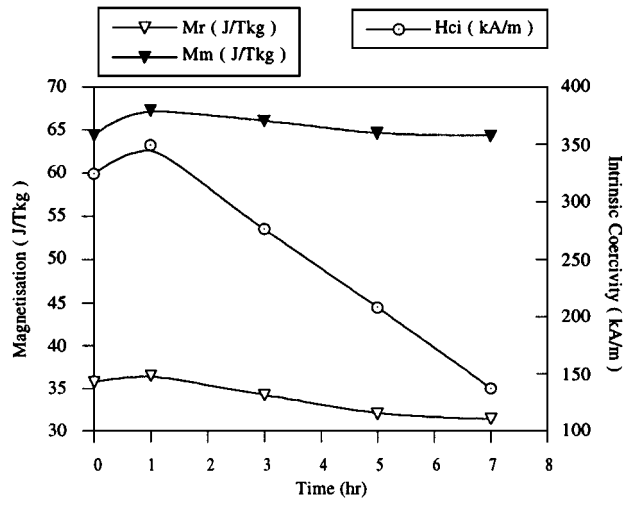

Figure 2 Magnetic properties of conventionally synthesized strontium hexaferrite powders hydrogenated at 850 °C under 1.3 bar initial pressure for different times and then calcined at 1000 °C for 1 h in air. (Typical error: remanence ±3%, coercivity ±2%).

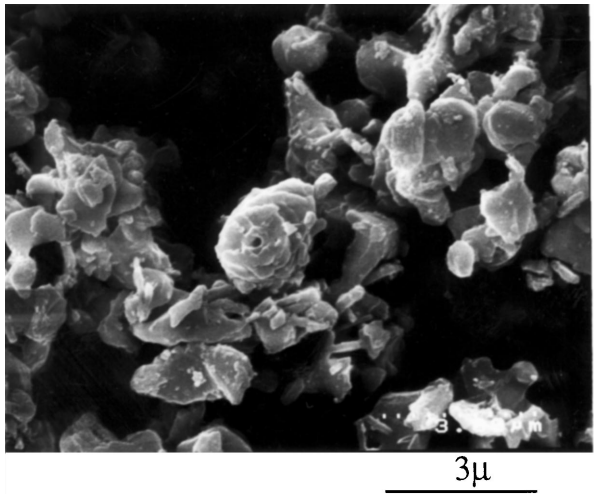

Figure 3 HRSEM micrograph of conventionally synthesized hexaferrite powder hydrogenated at 850 °C under an initial pressure of 1 bar for 1 h.

increasing time up to 1 h and then decreases linearly and rapidly for longer times.

It seems that, on increasing the time of hydrogenation, the extent of reduction increased, leading to a corresponding increase in the proportion of fine sub-grains. Consequently, better magnetic properties were obtained after re-calcination. Increasing the hydrogenation time beyond the optimum point (i.e., 1 h) resulted, however, in a coarsening of the pre-formed substructure that was probably responsible for the subsequent decrease in the coercivity. The microstructures of the powders hydrogenated for 1 and 7 h are shown in Fig. 3 and Fig. 4, respectively. These micrographs tend to confirm that increasing the hydrogenation time coarsens the subgrain size, producing larger grains after re-calcination.

3.3. Optimized initial hydrogenation pressure

The results of the XRD and magnetic measurements on the powders hydrogenated at 850 °C for 1 h under different initial pressures, followed by re-calcination at 1000 °C for 1 h in air, are shown in Fig. 5 and Fig. 6, respectively.

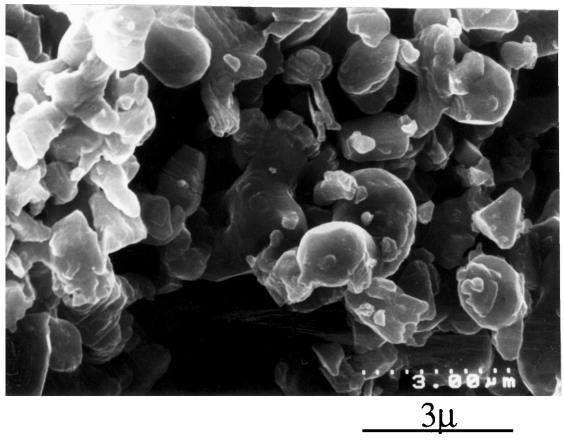

Figure 4 HRSEM micrograph of conventionally synthesized hexaferrite powder hydrogenated at 850 °C under an initial pressure of 1 bar for 7 h.

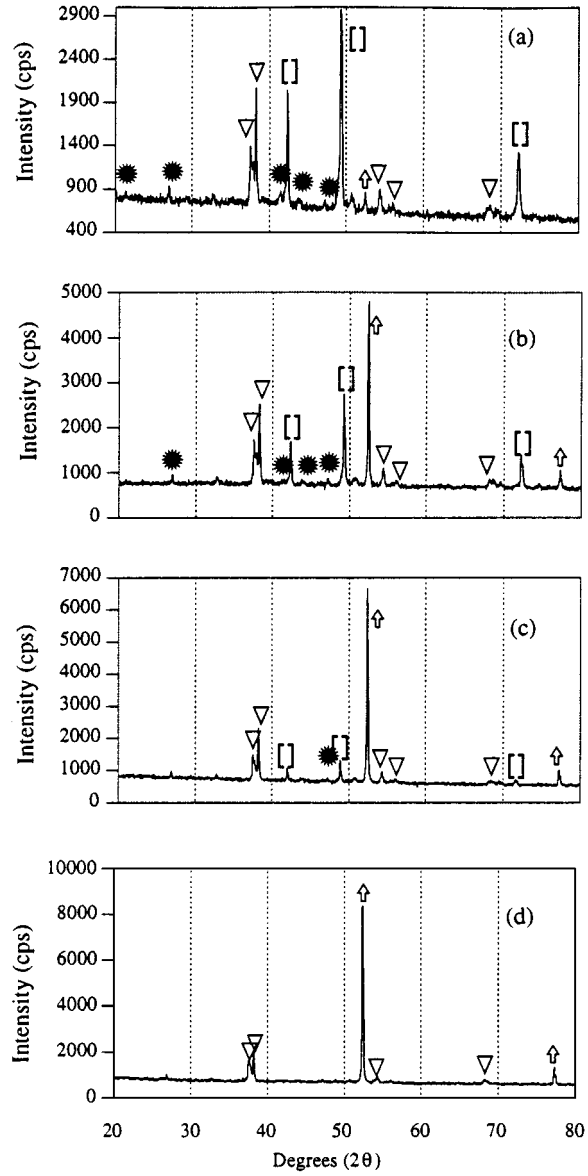

Figure 5 XRD traces for the conventionally synthesized strontium hexaferrite powders hydrogenated at 850 °C under different initial pressures: (a) 0.25 bar; (b) 0.5 bar; (c) 1 bar; and (d) 1.3 bar (⇧ = Fe, ∇ = $Sr_7Fe_{10}O_{22}$, [] = FeO, ✸ = Sr-hexaferrite).

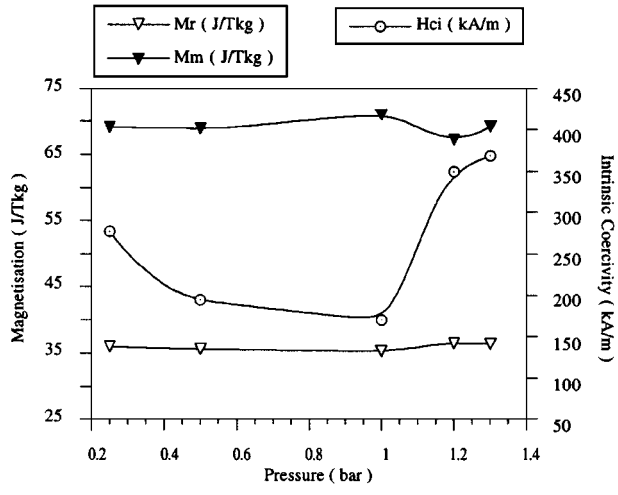

Figure 6 Magnetic properties of the conventionally synthesized strontium hexaferrite powders hydrogenated at 850 °C for 1 h under different initial pressures and re-calcined at 1000 °C for 1 h in air. (Typical error: remanence ±3%, coercivity ±2%).

It can be seen that, with increasing hydrogen pressure, the degree of reduction increased to completion at 1.3 bar. At 0.25 bar initial pressure (Fig. 5a), the peaks due to Fe are very weak while FeO exhibits the strongest peaks [7, 8]. It shows that the reduction of Fe_2O_3 has passed the Fe_3O_4, i.e., $Fe_2O_3 \cdot FeO$ stage [9, 10]. However, despite the formation of Fe, FeO, and $Sr_7Fe_{10}O_{22}$, the hexaferrite phase is still present [11, 12]. At 0.5 bar initial pressure (Fig. 5b), the peaks due to the hexaferrite phase and FeO have decreased, whereas the peaks due to Fe have increased. At 1 bar initial pressure (Fig. 5c), only very weak traces of the hexaferrite and FeO phases are present. Finally, in Fig. 5d, at 1.3 bar initial pressure, the peaks for both the hexaferrite and FeO have disappeared completely, indicating that the reduction process is complete.

Fig. 6 shows that the M_r and M_m were relatively constant as a function of increasing H_2 pressure. However, the H_{ci} decreased with increasing initial pressure from 0.25 bar to 1 bar and then exhibited significant increase with pressure up to 1.3 bar. The decrease in the H_{ci} values up to 1 bar initial pressure could be due to the presence of some residual large grains of hexaferrite that did not decompose fully during hydrogenation. This is indicated by the sharp increase in H_{ci}, which coincides with the disappearance of the residual hexaferrite phase at initial pressures above 1 bar (see Fig. 5). The increase in coercivity on hydrogenating at an initial pressure above 1 bar can be attributed to the finer grain size present after re-calcination, which is due to the transformation of the single-crystal particles into smaller grains during hydrogenation, forming polycrystalline particles. The highest intrinsic coercivity of around 368 kA/m was thus obtained at 1.3 bar initial pressure.

The magnetization curves of the samples, hydrogenated under 0.25 bar, 0.5 bar, 1 bar, and 1.3 bar initial pressure, are shown in Fig. 7a, b, c, and d, respectively, together with the curves obtained after the re-calcination treatment. It is very interesting to note that with increasing pressure, as the degree of reduction and hence proportion of Fe in the hydrogenated samples increased, so did the M_m, while in the re-calcined samples, the shape of initial magnetization curve exhibited a considerable reduction in the initial susceptibility, which is indicative of single-domain behavior.

Fig. 8 shows the temperature and pressure as functions of the time of hydrogenation of the powders for different initial hydrogenation pressures. It can be seen that, with increasing temperature, the pressure increased slightly due to the thermal expansion of the gas but after about 100 min and at temperatures between 850–950 °C, it dropped dramatically as hydrogen absorption occurred. As the temperature was decreased, the degree of absorption reduced and eventually stopped. However, at an initial pressure of 0.25 bar, there was a small increase in pressure between 200 and 300 min, which was attributed to expansion of H_2O vapor, produced as a by-product of the reduction process that was not completed at a relatively high temperature. The overall pressure reduction from the initial gas pressure in each figure is indicative of the degree of reduction. Comparing Fig. 5 to Fig. 8 in terms of the

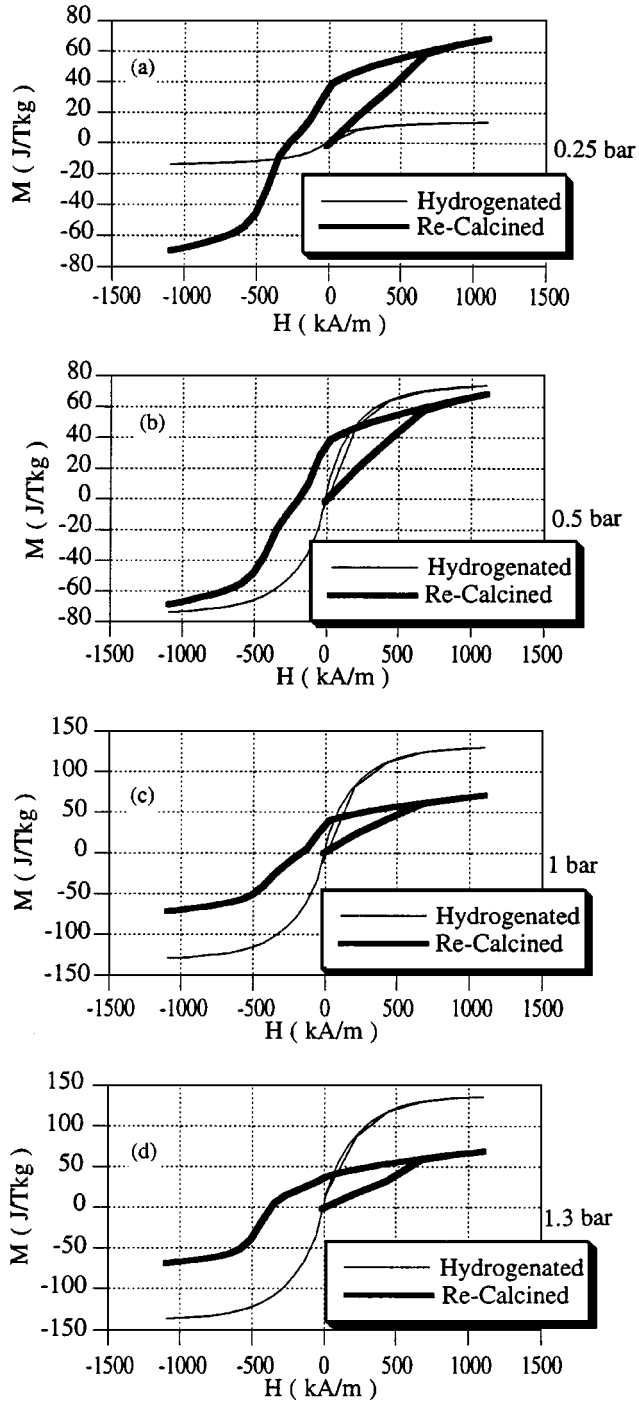

Figure 7 Magnetization curves of the samples hydrogenated under (a) 0.25 bar; (b) 0.5 bar; (c) 1 bar; and (d) 1.3 bar initial pressures at 850 °C for 1 h and re-calcined at 1000 °C for 1 h.

phases formed under different initial gas pressure conditions, indicates that the minimum pressure reduction required for the formation of FeO is around 200 mbar (Fig. 8a), while for the onset of Fe formation it is about 400 mbar (Fig. 8b), whereas for the complete formation of Fe it is around 700 mbar (Fig. 8d).

3.4. Optimized hydrogenation temperature

After hydrogenation at 700 °C for 1 h, under an initial pressure of 1.3 bar, the color of the sample became greenish and its magnetic properties changed radically.

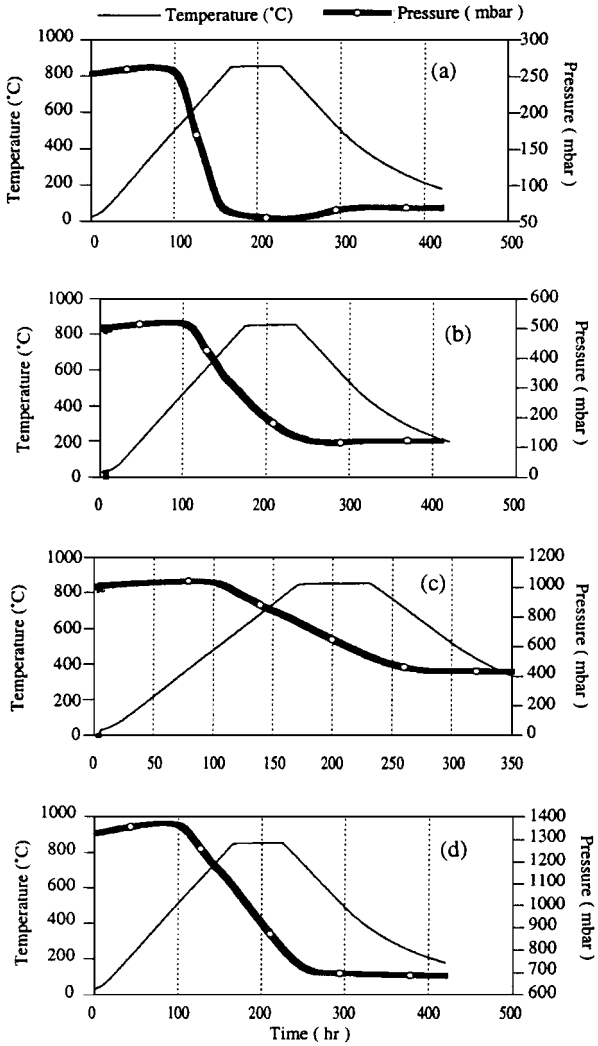

Figure 8 Temperature and hydrogen pressure as a function of time for a conventionally synthesized strontium hexaferrite powder hydrogenated at 850 °C under different initial pressures: (a) 0.25 bar; (b) 0.5 bar; (c) 1 bar; and (d) 1.3 bar.

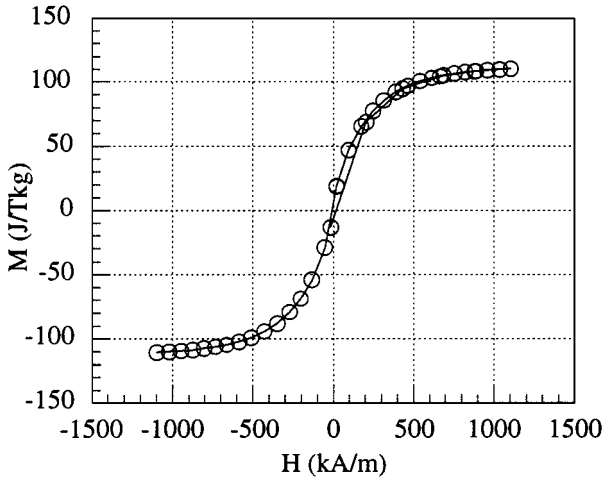

Figure 9 Magnetization curve of the initial powder, hydrogenated under 1.3 bar initial pressure at 700 °C for 1 h, showing very low remanence and intrinsic coercivity but much higher maximum magnetization.

As indicated in Fig. 9 and Table I, the M_r and H_{ci} decreased markedly to values close to zero. However, the magnetization increased considerably and approached complete saturation with a value of ~ 110 J/Tkg.

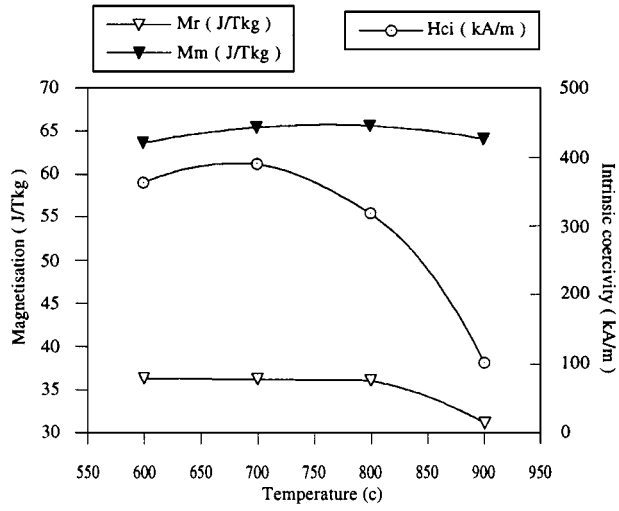

Figure 10 Magnetic properties of the conventionally synthesized strontium hexaferrite powder hydrogenated for 1 h under initial pressure of 1.3 bar at different temperatures and then re-calcined at 1000 °C for 1 h in air. (Typical error: remanence ±3%, coercivity ±2%)

The magnetic properties of the conventionally synthesized hexaferrite powder, hydrogenated under 1.3 bar initial pressure for 1 h at different temperatures and re-calcined at 1000 °C for 1 h in air, are summarized in Fig. 10.

The M_m again changes negligibly with temperature between 600 and 900 °C, while the M_r shows only a small decrease above 800 °C. It can thus be concluded that the main effect of the hydrogenation and recalcination processes is to alter the coercivity, leaving the remanence and maximum magnetization essentially unchanged. The intrinsic coercivity increased with increasing hydrogenation temperature up to 700 °C and then decreased dramatically. The increase in the H_{ci} up to a value of 391 kA/m at 700 °C can be attributed to the extent of the reduction process and to the formation of a fine microstructure. Above 700 °C, grain growth resulted in the decrease in the intrinsic coercivity as well as the remanence due to a lower squareness factor.

This is confirmed by comparing Figs. 11 and 12, which correspond to the hydrogenation treatment at

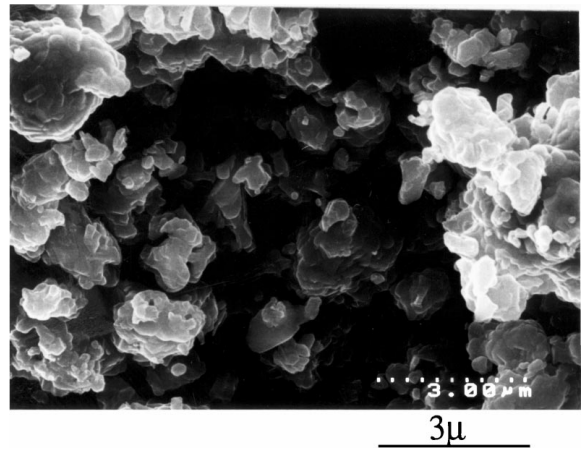

Figure 11 HRSEM micrograph of the conventionally synthesized hexaferrite powder hydrogenated at 700 °C under an initial pressure of 1.3 bar for 1 h and then re-calcined at 1000 °C for 1 h, showing very small ferrite grains.

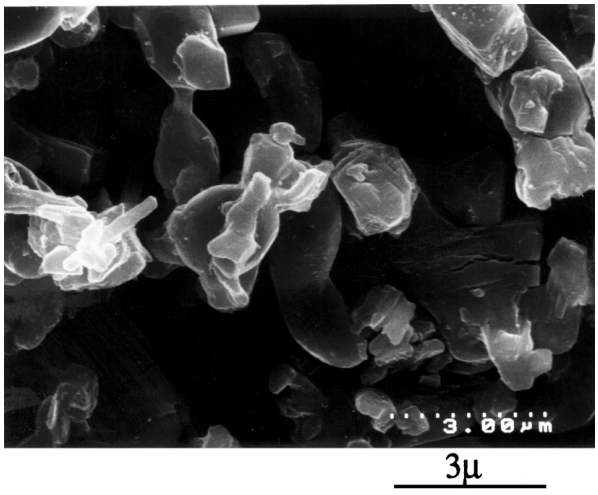

Figure 12 HRSEM micrograph of the conventionally synthesised hexaferrite powder hydrogenated at 900 °C under an initial pressure of 1.3 bar for 1 h.

700 and 900 °C respectively. It can be seen that the microstructure of the sample hydrogenated at 700 °C is much finer. Hence, the optimum hydrogenation temperature is close to 700 °C at this hydrogen pressure.

The XRD traces of powders hydrogenated at 700 and 900 °C are shown in Fig. 13a and b, respectively. In Fig. 13a, traces due to FeO are visible, indicating that only partial reduction of iron oxide has occurred at 700 °C, in contrast to the absence of peaks for FeO, indicating that full reduction occurred at 900 °C. These observations indicate that the finer sub-grain size is achieved prior to full reduction.

3.5. Optimized re-calcination temperature

The magnetic properties of conventionally synthesised hexaferrite powders hydrogenated under optimum

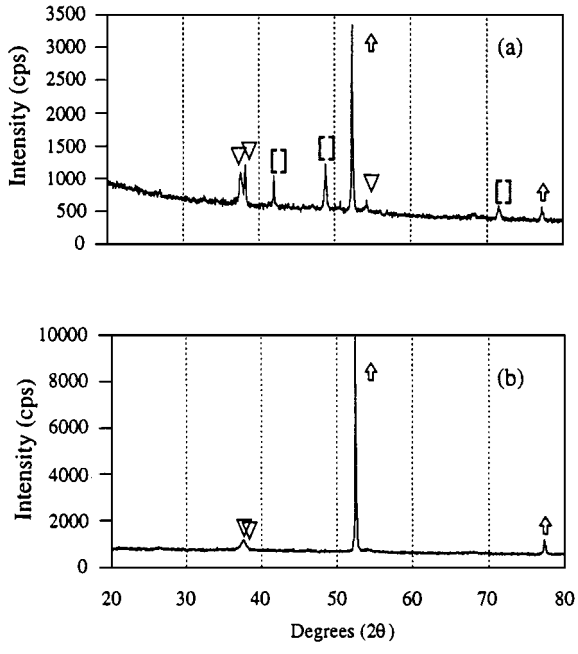

Figure 13 XRD traces of the conventionally synthesized strontium hexaferrite powder hydrogenated under 1.3 bar initial pressure for 1 h at: (a) 700 °C and (b) 900 °C (⇧ = Fe, ∇ = $Sr_7Fe_{10}O_{22}$, [] = FeO).

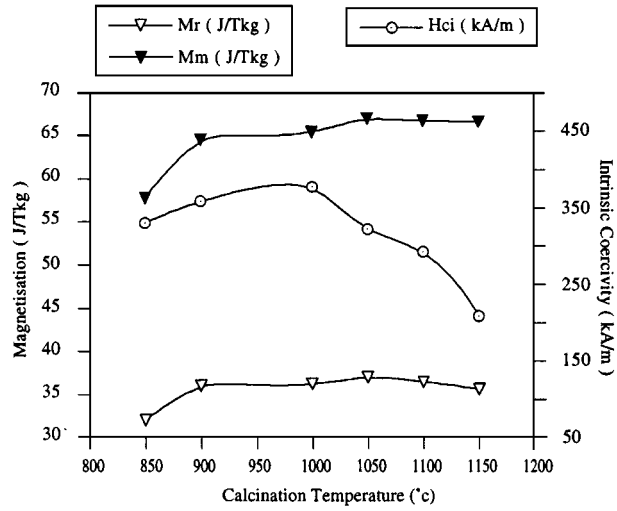

Figure 14 Magnetic properties of the conventionally synthesized strontium hexaferrite powder hydrogenated at 700 °C for 1 h under an initial pressure of 1.3 bar and re-calcined at different temperatures for 1 h in air. (Typical error: remanence ±3%, coercivity ±2%)

conditions and then re-calcined at different temperatures for 1 h in air are shown in Fig. 14.

It can be seen that the M_r and M_m increased with increasing re-calcination temperature up to about 900–1000 °C and thereafter remained almost constant. This means that the oxidation process, causing the reformation of ferrite phase, is completed within this temperature range. The lower magnetic properties prior to this point can be ascribed to the presence of some intermediate phases with poorer magnetic properties. This is in contrast to the intrinsic coercivity, which after increasing with increasing re-calcination temperatures up to about 1000 °C, decreases rapidly to below the value (at 850 °C). This is attributed to the grain growth occurring at temperatures above 1000 °C, as evidenced by comparing Figs 11 and 15, which correspond to re-calcination for 1 h at temperatures of 1000 and 1150 °C, respectively.

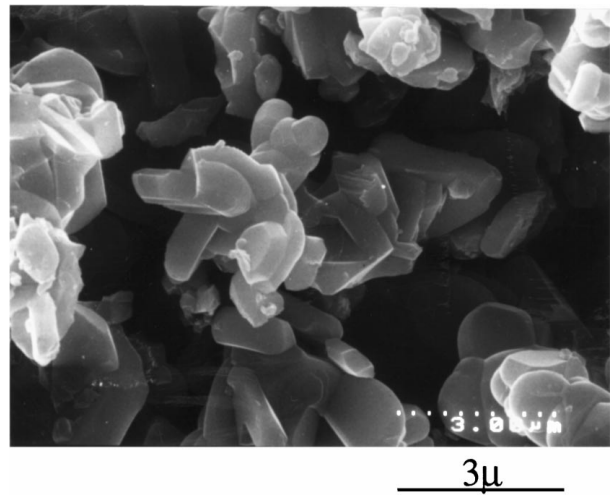

Figure 15 HRSEM micrograph of the conventionally synthesized hexaferrite powder hydrogenated at 700 °C under an initial pressure of 1.3 bar for 1 h and then re-calcined at 1150 °C for 1 h, showing the formation of large ferrite grains at high re-calcination temperatures.

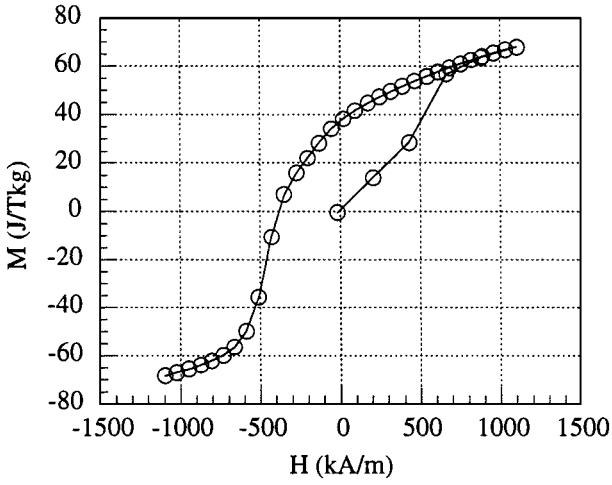

Figure 16 Magnetization curve of the hydrogenated powder, re-calcined at 1000 °C for 1 h in air, showing a remanence similar to the initial value and an increased coercivity.

3.6. Effect of optimized hydrogenation and re-calcination

When the powder optimally hydrogenated at 700 °C for 1 h was then optimally re-calcined at 1000 °C for 1 h in air, the color changed to black and the magnetic measurements showed some significant differences from those of the initial powder. As can be seen in Fig. 16 and Table I, the remanence and saturation magnetization had values close to the initial values, but the intrinsic coercivity exhibited an increase of $\sim 20\%$ compared to the initial value.

The XRD traces for the as-synthesised powder, the optimally hydrogenated powder, plus the optimally hydrogenated and re-calcined powder are shown in Fig. 17. All the peaks in Fig. 17a belong to the stoichiometric M-type strontium hexaferrite, $Sr_6Fe_{12}O_{19}$ or $SrO \cdot 6Fe_2O_3$ [12]. Thus, the initial powder consisted predominantly of the strontium hexaferrite phase.

The XRD traces in Fig. 17b show that a radical change in the phase constitution occurred during hydrogenation. There are almost no traces of the hexaferrite phase, and the main peaks can now be ascribed to Fe, FeO, and $Sr_7Fe_{10}O_{22}$ ($7SrO \cdot 5Fe_2O_3$) [7, 8, 11, 13]. The amount of α-Fe was around 51%, by weight, obtained by comparing the M_m value for the hydrogenated powder with that for pure α-Fe ($M_m = 218$ J/Tkg at 293 K [14]). These results show that, during hydrogenation, the strontium hexaferrite was decomposed into $7SrO \cdot 5Fe_2O_3$ and Fe_2O_3 and the resultant Fe_2O_3 was then reduced by the hydrogen to form α-Fe. The water that remained in the hydrogen furnace after these processes confirmed the reaction of oxygen with hydrogen.

Thus, the very high maximum magnetization and very low intrinsic coercivity achieved during this stage of the process (Fig. 9) can be attributed to the significant presence of the magnetically soft α-Fe phase. The presence of FeO after hydrogenation indicated only partial reduction of Fe_2O_3 to Fe by hydrogen. However, the reduction stages from Fe_2O_3 to Fe_3O_4 and subsequently to FeO were definitely completed. The phases indicated in Fig. 17b are the main phases present, although there

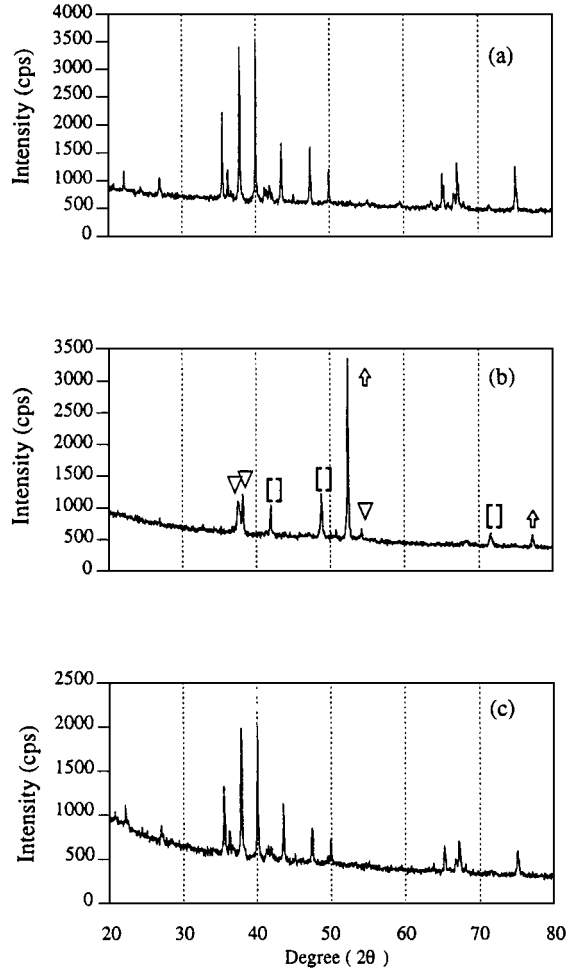

Figure 17 XRD patterns of (a) initial powder; (b) hydrogenated at 700 °C for 1 h under initial pressure of 1.3 bar; and (c) subsequently calcined at 1000 °C for 1 h in air (⇧ = Fe, ∇ = $Sr_7Fe_{10}O_{22}$, [] = FeO).

were also a few weak peaks, attributed to intermediate phases, of which the more probable ones are $Sr_3Fe_2O_7$, $2SrO \cdot Fe_2O_3$ ($Sr_2Fe_2O_5$) [15, 17].

In Fig. 17c, only the strontium ferrite peaks were observed, indicating that, after subsequent re-calcination, the reduction reactions were completely reversed. The close similarity of the remanence and maximum magnetization values for the initial and final powders confirms this observation (see Table I).

The TMA results were also consistent with the XRD observations. The TMA curves for the three powders with their corresponding derivatives are shown in Fig. 18.

The strontium ferrite curve in Fig. 18a exhibits a slope change (i.e., trough in the dM/dT curve) at 440 °C (±20 °C), which is close to the reported Curie point of this phase of 470 ± 10 °C [18]. This change is no longer visible in Fig. 18b as the ferrite phase is absent, but it could be seen again after the re-calcination (Fig. 18c). It appears that the slope change in this figure occurred at 430 °C, i.e., 10 °C less than that of the initial powder. Another prominent slope change occurred in all the runs at around 130 °C and this was due to the magnetic contribution of the sample holder that acts as an internal calibration.

The morphologies of the powders are exhibited in Figs 19 to 22.

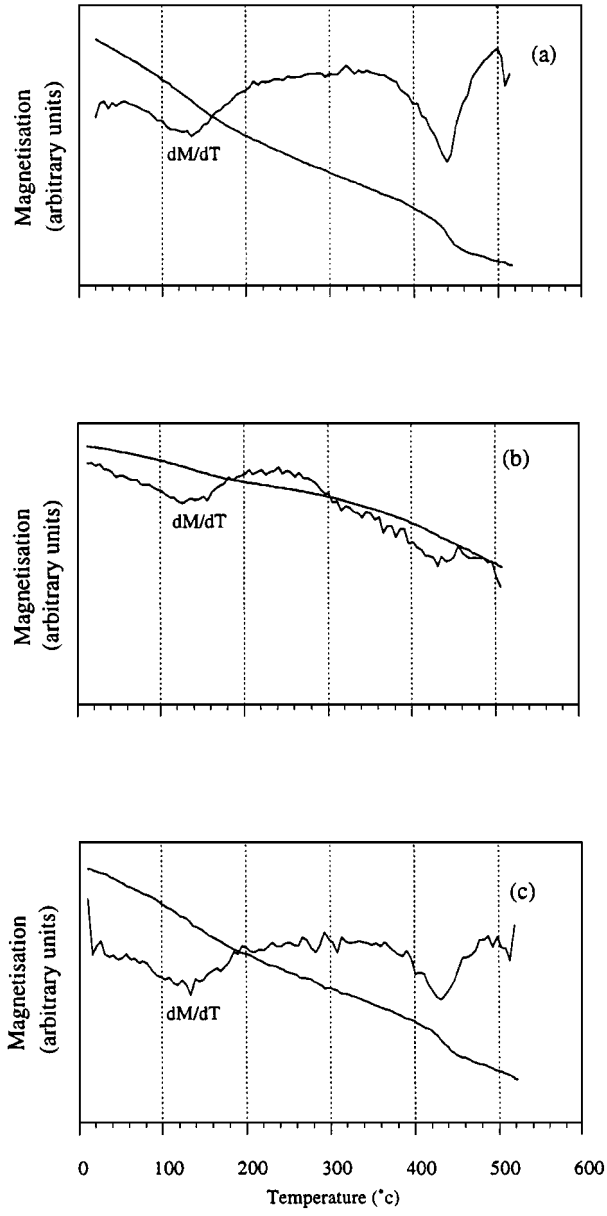

Figure 18 TMA and dM/dT curves of (a) initial powder; (b) hydrogenated at 700 °C for 1 h under initial pressure of 1.3 bar; and (c) subsequently calcined at 1000 °C for 1 h in air.

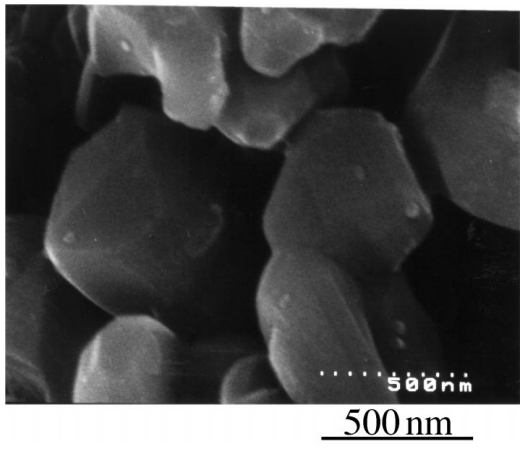

Figure 19 HRSEM micrograph of initial as-conventionally synthesized powder.

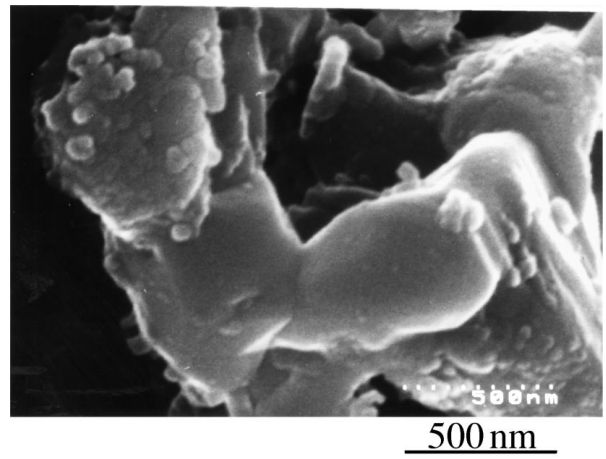

Figure 20 HRSEM micrograph of hexaferrite powder after hydrogenation at 700 °C for 1 h under initial 1.3 bar pressure, indicating a very fine substructure at the top left-hand corner.

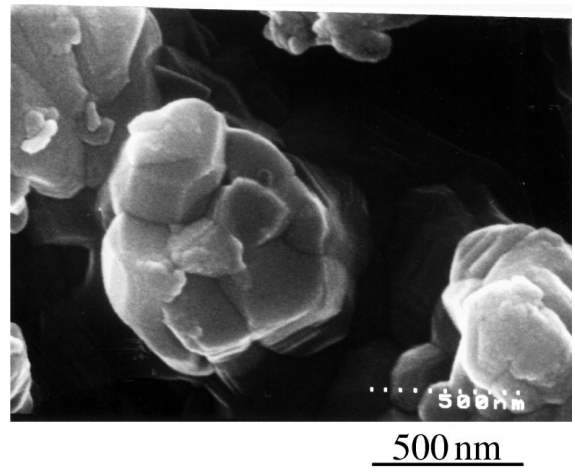

Figure 21 HRSEM micrograph of hexaferrite recovered during subsequent re-calcination at 1000 °C in air after hydrogenation at 700 °C for 1 h under initial 1.3 bar pressure. The smaller grains appear within what was originally an individual particle.

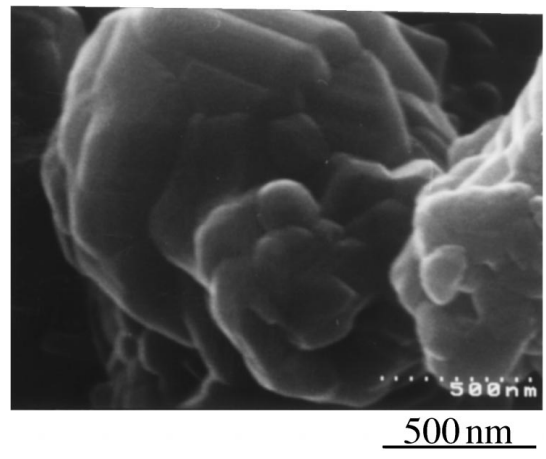

Figure 22 HRSEM micrograph of hexaferrite recovered during subsequent re-calcination at 1000 °C for 1 h in air after hydrogenation at 700 °C for 1 h under initial 1.3 bar pressure, showing some degree of inter-particle neck growth.

Fig. 19 shows the hexagonal grains of the initial hexaferrite powder. The surfaces of the grains are smooth, and the grains edges are sharp. The mean grain size in this powder was below 500 nm.

In Fig. 20, it can be seen that some of the original grains after optimal hydrogenation now comprise very fine sub-grains (see top left-hand corner). The mean size of these sub-grains was below 100 nm.

Fig. 21 shows that the optimally hydrogenated hexaferrite particle sub-grains after optimum re-calcination are much finer than those of the initial powder (Fig. 19). The original individual particles now appear to be subdivided into finer grains. The mean size of the grains shown in Fig. 21 was below 300 nm.

The increased intrinsic coercivity of the re-calcined powder (Fig. 16) as compared to that of the initial powder (Fig. 1) can be attributed to this finer structure. Regarding the size of grains shown in Fig. 21, they are much smaller than the single domain size for Sr–hexaferrite (1 μm). The shape of the initial magnetization curves in Figs 1 and 16 also support this finding. The initial susceptibility indicated in Fig. 16 is much lower than that of the initial powder shown in Fig. 1. It also appears that the re-calcination process produces some degree of inter-particle neck growth as indicated in Fig. 22.

4. Conclusions

The results of this investigation show that, while the values of remanence and maximum magnetization after re-calcination are almost the same as those of the initial material, i.e., before hydrogenation, the effect of the hydrogenation and re-calcination treatments is to increase the coercivity. With increasing temperature/initial pressure and/or time of hydrogenation, the increased degree of reduction and consequent formation of a large number of fine sub-grains results in magnetic behavior approaching that characteristic of single-domain material and, therefore, higher coercivities after re-calcination. However, beyond an optimum point, any further increase in the hydrogenation time and/or temperature leads to marked grain growth and hence a decrease in the coercivity. Thus, it is very important to note that the optimum point for maximizing the formation of fine sub-grains does not necessarily correspond to the point of complete reduction. Furthermore, the optimum re-calcination temperature is that which is high enough for the re-formation of the hexaferrite phase but not so high that undesirable grain growth occurs. The highest coercivity was around 400 kA/m, obtained for a powder hydrogenated at 700 °C for 1 h under an initial pressure of 1.3 bar, followed by re-calcination in air at 1000 °C for 1 h.

Acknowledgements

Thanks are due to the members of the Applied Alloy Chemistry Group (School of Metallurgy and Materials) for their co-operation. The financial support of Tehran University is gratefully acknowledged.

References

1. S. KITAHATA and M. KISHIMOTO, *IEEE Transactions on Magnetics* **6** (1994) 4107.
2. Y. K. HONG, H. S. JUNG, N. P. HUR and S. MATAR, *J. Phys. IV* **7** (1997) C1 329.
3. A. ATAIE, I. R. HARRIS and C. B. PONTON, Patent Application No. PCT/GB95/02758, November 1995.
4. A. ATAIE, C. B. PONTON and I. R. HARRIS, *J. Mat. Sci.* **20** (1996) 5521.
5. S. A. S. EBRAHIMI, A. J. WILLIAMS, N. MARTINEZ, A. ATAIE, A. KIANVASH, C. B. PONTON and I. R. HARRIS, *J. Phys. IV* **7** (1997) C1 325.
6. N. MARTINEZ, S. A. S. EBRAHIMI, A. J. WILLIAMS and I. R. HARRIS, *J. Mat. Sci.* (1999) in press.
7. H. E. SWANSON, NBS Circular 539, **4** (1955) 3; JCPDS/6-0696.
8. T. YAGI, T. SUZUKI and A. AKIMOTO, *J. Geophys. Res.* **90** (1985) 8784; JCPDS/39-1088.
9. National Bureau of Standards (U.S) Monogr. 25, 18 (1981) 37; JCPDS/33-664.
10. *Idem., ibid.* (1967) 31; JCPDS/19-629.
11. E. LUCCHINI, D. MINICHELLI and G. SLOCCARI, *J. Am. Ceram. Soc.* **57** (1974) 42; JCPDS/26-980.
12. V. ADELSKOLD, *Arkive for Kemi, Min. Geol.* **12A** (1938) 1; JCPDS/24-1207.
13. R. BIRISI, *Ann. Chim. (Rome)* **59** (1969) 385; JCPDS/22-1427.
14. B. D. CULLITY, "Introduction to Magnetic Materials" (Addison-Wesley, 1972).
15. S. DANN, D. CURRIE and M. WELLER, *J. Solid State Chem.* **97** (1992) 179; JCPDS/45-398.
16. J. BEREKTA and T. BROWN, *Aust. J. Chem.* **24** (1971) 237; JCPDS/28-1227.
17. S. SHIN, *Mater. Res. Bull.* **13** (1978) 1017; JCPDS/33-677.
18. L. JAHN and H. G. MULLER, *Phys. Status Solidi* **35** (1969) 723.

Received 19 June
and accepted 6 August 1998